International Journal of Mathematical Research
2015 Vol.4, No.1, pp.27-41
ISSN(e): 2306-2223
ISSN(p): 2311-7427
DOI: 10.18488/journal.24/2015.4.1/24.1.27.41

A STEADY MHD BOUNDARY-LAYER FLOW OF WATER-BASED NANOFLUIDS OVER A MOVING PERMEABLE FLAT PLATE

Eshetu Haile[1]† --- B. Shankar[2]

[1,2]Department of Mathematics, Osmania University, Hyderabad, India

ABSTRACT

A steady boundary-layer flow of water based nanofluids over a moving permeable surface were analyzed. The plate was assumed to move in the same or opposite direction to the free stream. The model describing the flow regime characterizes the Sakiadis and Blasius flow scenarios. The PDEs in the governing equations were transformed into ODEs with the help of similarity transformations. The transformed equations were solved numerically by the shooting method with Runge-Kutta integration scheme. Effects of the governing parameters were thoroughly studied and explicitly explained graphically and in tabular form. Numerical results of the velocity field, temperature distribution, skin friction and Nusselt number were obtained. The results were compared with previous works and they are found in excellent agreement.

Keywords: Magnetic field, Boundary-layer flow, Moving surface, Water-based nanofluids, Steady flow, Permeable surface.

Received: 13 August 2014/ **Revised:** 17 September 2014/ **Accepted:** 20 September 2014/ **Published:** 23 September 2014

Contribution/ Originality

For further applications, new improvements of the models of Motsumi and Makinde [15] were made by including uniform magnetic field and Ohmic effects. Accordingly, the paper briefly explains effects of the various governing parameters on velocity and temperature profiles, skin friction and wall heat transfer rate for both Blasius and Sakiadis flow situations.

1. INTRODUCTION

Nanofluids are new class of heat transfer fluids which contain a base fluid and nanoparticles. They are characterized by an enrichment of a base fluid like Water, toluene, Ethylene glycol or oil with nanoparticles in variety of types like Metals, Oxides, Carbides, Carbon, etc. Today, nanofluids are sought to have wide range of applications in medical applications, biomedical industry, detergency, power generation in nuclear reactors and more specifically in any heat

† *Corresponding author*

removal involved industrial applications. The ongoing research ever since then has extended to utilization of nanofluids in microelectronics, fuel cells, pharmaceutical processes, hybrid-powered engines, engine cooling, vehicle thermal management, domestic refrigerator, chillers, heat exchanger, nuclear reactor coolant, grinding, machining, space technology, defense and ships, and boiler flue gas temperature reduction [1]. A comprehensive survey of convective transport in nanofluids has been made by Buongiorno [2] he gave satisfactory explanation for the abnormal increase of thermal conductivity and viscosity relative to the base fluid.

Many applications of MHD boundary layer flows of heat and mass transfer over flat surfaces are found in many engineering and geophysical applications such as geothermal reservoirs, thermal insulation, enhanced oil recovery, packed-bed catalytic reactors, cooling of nuclear reactors. Boundary layer flow of nanofluids over a moving surface in a flowing fluid was nicely explained by Bachok, et al. [3]. Moreover, Olanrewaju, et al. [4] also studied boundary layer flow of nanofluids over a moving surface in a flowing fluid in the presence of radiation. Ahmad, et al. [5] presented a numerical study on the Blasius and Sakiadis problems in nanofluids under isothermal condition. Hady, et al. [6] studied the Blasius and Sakiadis flow in a nanofluid through a porous medium in the presence of thermal radiation under a convective surface boundary condition. A study on boundary layer flow of a nanofluid past a stretching sheet with a convective boundary condition was conducted by Makinde and Aziz [7]. Khan, et al. [8] examined the unsteady free convection boundary layer flow of a nanofluid along a stretching sheet with thermal radiation and viscous dissipation effects in the presence of a magnetic field. Magnetic field effects on free convection flow of a nanofluid past a vertical semi-infinite flat plate was studied by Hamad, et al. [9]. Hamad and Pop [10] theoretically studied a similarity solution of the steady boundary layer flow near the stagnation-point flow on a permeable stretching sheet in a porous medium saturated with a nanofluid and in the presence of internal heat generation/absorption.

Thermal radiation effects have substantial applications in many industrial areas, such as electrical power generation, solar power technology and aerospace engineering. Hady, et al. [11] studied the flow and heat transfer characteristics of a viscous nanofluid over a nonlinearly stretching sheet in the presence of thermal radiation. Effects of a thin gray fluid on MHD free convective flow near a vertical plate with ramped wall temperature under small magnetic Reynolds number was studied by Rajesh [12]. Moreover, MHD Flow and heat transfer over stretching/shrinking sheets with external magnetic field, viscous dissipation and joule effects was studied by Jafar, et al. [13]. Heat transfer in a viscous fluid over a stretching sheet with viscous dissipation and internal heat generation was studied by Vajravelu and Hadjinicolaou [14].

The simultaneous effects of magnetic field, thermal radiation, viscous dissipation, ohmic effects and permeability of surfaces on heat transfer of nanofluids over a moving flat plate has been analyzed. Accordingly, the models and new improvements are presented in this work

extending the work of Motsumi and Makinde [15] to include uniform magnetic field and ohmic effect in the momentum and energy equations respectively, for further applications. The governing boundary layer equations are reduced to a system of ordinary differential equations by using similarity transformations. The transformed equations are solved numerically by using the shooting technique with Runge-Kutta integration scheme. The influence of the various governing parameters on the velocity profile, temperature profile, skin friction and Nusselt numbers are discussed in detail.

2. FORMULATION OF THE PROBLEM

We considered two dimensional steady laminar boundary layer flow of water-based nanofluids Cu-water and Al_2O_3-water over a flat permeable plate moving with a constant velocity U_w in the same or opposite direction to the free stream velocity $U_\infty = ax, a \neq 0$. The x-axis extends parallel to the plate surface while the y-axis extends normal to the surface. The flow field contains a uniform magnetic field, thermal radiation and viscous dissipation. The magnetic field is applied parallel to the y-axis. At the moving surface, the temperature takes a constant value T_w. Both the base fluid and the nanoparticles are assumed to be in thermal equilibrium and no slip occurs among them. Taking these conditions into account, the governing boundary layer equation of continuity, momentum and energy could be written in Cartesian coordinates x and y in dimensional form as of [3, 6, 15, 16]:

$$\frac{\partial u}{\partial x} + \frac{\partial v}{\partial y} = 0 \tag{1}$$

$$u\frac{\partial u}{\partial x} + v\frac{\partial u}{\partial y} = \frac{\boldsymbol{\mu_{nf}}}{\rho_{nf}}\frac{\partial^2 u}{\partial y^2} - \frac{\sigma {B_0}^2}{\rho_{nf}}u, \tag{2}$$

$$\frac{\partial T}{\partial x} + v\frac{\partial T}{\partial y} = \alpha_{nf}\frac{\partial^2 T}{\partial y^2} + \frac{\mu_{nf}}{(\rho C_p)_{nf}}\left(\frac{\partial u}{\partial y}\right)^2 + \frac{\sigma {B_0}^2}{(\rho C_p)_{nf}}u^2 - \frac{1}{(\rho C_p)_{nf}}\frac{\partial q_r}{\partial y}, \tag{3}$$

where (u, v) are the velocity components of the nanofluids in the x and y directions, respectively; T is temperature and T_∞ is the ambient temperature; B_0 is the applied uniform magnetic field; σ is the electrical conductivity of the base fluid; α_{nf}, $(\rho C_p)_{nf}$, ρ_{nf} and μ_{nf} are the thermal diffusivity, heat capacity, density and dynamic viscosity of the nanofluid, respectively. According to [6] and [17], these fluid properties are given by: $\mu_{nf} = \frac{\mu_f}{(1-\emptyset)^{2.5}}$, $\nu_f = \frac{\mu_f}{\rho_f}$, $\rho_{nf} = (1-\emptyset)\rho_f + \emptyset\rho_s$,

$$\alpha_{nf} = \frac{k_{nf}}{(\rho C_p)_{nf}}, \quad k_{nf} = k_f\left(\frac{k_s + 2k_f - 2\emptyset(k_f - k_s)}{k_s + 2k_f + \emptyset(k_f - k_s)}\right) \text{ and } (\rho C_p)_{nf} = (1-\emptyset)(\rho C_p)_f + \emptyset(\rho C_p)_s, \tag{4}$$

where μ_f, ρ_f and ν_f are the dynamic viscosity, density and kinematic viscosity of the base fluid and k_{nf} is thermal conductivity of the nanofluid; ρ_s and $(\rho C_p)_s$ are the density and heat capacitance of the nanoparticles, respectively; $\emptyset$ is the nanoparticle volume fraction.

According to the Rosseland diffusion approximation of Raptis [18] and Hossain and Takhar [19] the radiative heat flux q_r is given by

$$q_r = -\frac{4\sigma^*}{3k^*}\frac{\partial T^4}{\partial y}, \tag{5}$$

where k^* and σ^* are the Rosseland mean absorption coefficient and the Stefan-Boltzmann constant, respectively. We assume that the temperature differences within the flow are sufficiently small such that T^4 may be expressed as a linear function of temperature,

$$T^4 \approx 4T_\infty^3 T - 3T_\infty^4 . \tag{6}$$

Consider a variable plate surface permeability function V_w which is defined by

$$V_w(x) = -\frac{f_w}{2}\sqrt{\frac{U\upsilon_f}{x}}, \tag{7}$$

where $U = U_w + U_\infty$ and f_w is a constant with the properties

- $f_w > 0$ represents the transpiration (suction) rate at the plate surface,
- $f_w < 0$ corresponds to injection, and
- $f_w = 0$ is considered for an impermeable surface.

The boundary conditions to the differential equations are:

$$\begin{aligned} &u(x,0) = U_w\,,\ v(x,0) = V_w(x),\ T(x,0) = T_w\,, \\ &u(x,\infty) = U_\infty,\ T(x,\infty) = T_\infty\,. \end{aligned} \tag{8}$$

Let us introducing the similarity variables

$$\begin{cases} \eta = \left(\frac{U}{x\upsilon_f}\right)^{\frac{1}{2}} y = \frac{y}{x}\sqrt{Re_x}, \\ T = T_\infty + (T_w - T_\infty)g(\eta), \\ \psi = \left(xU\upsilon_f\right)^{\frac{1}{2}} f(\eta). \end{cases} \tag{9}$$

The stream function ψ with $u = \frac{\partial \psi}{\partial y}$ and $v = -\frac{\partial \psi}{\partial x}$ result $u = Uf'(\eta)$ and $v = \frac{1}{2}\left(\frac{U\upsilon_f}{x}\right)^{1/2}(\eta f' - f)$; the stream function obviously satisfies the continuity equation (1). The substitution of equation (9) to the governing equations (2) and (3) reduce the PDEs to the following non-linear coupled ODEs:

$$f''' + \emptyset_1\left(\frac{1}{2}f\,f'' - \frac{Ha}{\emptyset_2}f'\right) = 0, \tag{10}$$

$$\left(\frac{knf}{kf} + \frac{4}{3R}\right)g'' + \emptyset_3\left(\frac{1}{2}Prfg' + \frac{Br}{\emptyset_4}f''^2\right) + Br.Ha.f'^2 = 0, \tag{11}$$

where η is the similarity variable, f is the dimensionless stream function and g is the dimensionless

temperature. The physical quantities which are expressible in terms of the nanoparticle volume fraction $\emptyset$ are given by:

$\emptyset_1 = (1-\emptyset)^{2.5}\left[1-\emptyset+\emptyset\left(\frac{\rho_s}{\rho_f}\right)\right]$, $\emptyset_2 = 1-\emptyset+\emptyset\left(\frac{\rho_s}{\rho_f}\right)$, $\emptyset_3 = 1-\emptyset+\emptyset\frac{(\rho C_p)_s}{(\rho C_p)_f}$ and

$\emptyset_4 = (1-\emptyset)^{2.5}\left[1-\emptyset+\emptyset\frac{(\rho C_p)_s}{(\rho C_p)_f}\right]$.

The corresponding boundary conditions become:

$$f(0) = fw,\ f'(0) = 1-r,\ g(0) = 1,\ f'(\eta)\to r,\ g(\eta)\to 0,\quad \text{as}\ \eta\to\infty. \tag{12}$$

The parameters introduced in the governing equations are defined by $r = \frac{U_\infty}{U}$ (Velocity ratio parameter), $Pr = \frac{\upsilon_f}{\alpha_f}$ (Prandtl number), $Ha = \frac{x}{U}\frac{\sigma B_0^2}{\rho_f}$(magnetic parameter), $Br = Pr.Ec = \frac{\mu_f U_\infty^2}{k_f(T_w - T_\infty)}$ (Brinkmann number) and $R = \frac{k^* k_f}{4\sigma^* T_\infty^3}$ (Radiation parameter). If we set $\emptyset = 0$, then we obtain the conventional fluid flow situations is recovered. The cases $r = 1$ ($U_w = 0$) and $r = 0$ ($U_\infty = 0$) are respectively the Blasius and Sakiadis flat plate flow scenarios. If $0.5 < r < 1$, the nanofluid motion is faster than that of the plate while if $0 < r < 0.5$ the plate is moving faster than the nanofluid. On the other hand, if $r > 1$, the fluid and the plate move in opposite directions as mentioned by Motsumi and Makinde [15].

Now, we are interested to study the skin-friction coefficient C_f and the local Nusselt numberNu_x.The parameters respectively characterize the surface drag and wall heat transfer rate. These quantities are defined by:

$$C_f = \frac{\tau_w}{\rho_f U_\infty^2} \quad \text{and} \quad Nu_x = \frac{x q_w}{k_f(T_w - T_\infty)} \tag{13}$$

where τ_w and q_w are the skin friction and heat flux at the surface, respectively as specified by Haile and Shanker [20] are given by:

$$\tau_w = \mu_{nf}\left(\frac{\partial u}{\partial y}\right)_{y=0} \text{ and } q_w = -\left(k_{nf} + \frac{16\sigma T_\infty^3}{3k^*}\right)\left(\frac{\partial T}{\partial y}\right)_{y=0}. \tag{14}$$

Using (13) and (14), the dimensionless skin friction coefficient (surface drag) and wall heat transfer rate become:

$$(Re_x)^{1/2} C_f (1-\emptyset)^{2.5} = f''(0) \text{ and } (Re_x)^{-1/2} Nu_x = -\left(\frac{k_{nf}}{k_f} + \frac{4}{3R}\right) g'(0) \tag{15}$$

where $Re_x = \frac{xU}{\upsilon_f}$ is the local Reynolds number. According to Bachok, et al. [3], $\frac{Nu_x}{\sqrt{Re_x}}$ represents the reduced Nusselt number and it is denoted by $-g'(0)$.

3. NUMERICAL SOLUTION

As equations (10) and (11) are non-linear ODEs, it is difficult to get the closed form solutions. As a result of this, the equations with the boundary conditions (12) are solved numerically using the shooting technique along with the fourth order Runge-Kutta integration scheme.

The conversion of the boundary value problem into an initial value problem is as follows:

If we let $f_1 = f,\ f_2 = f_1',\ f_3 = f'_2,\ f_4 = g$ and $f_5 = g'$, then we have

$$f'_3 = f''' = \emptyset_1\left(\frac{Ha}{\emptyset_2}f_2 - \frac{1}{2}f_1 f_3\right), \tag{16}$$

$$f'_5 = g'' = -\frac{1}{\left(\frac{k_{nf}}{k_f}+\frac{4}{3R}\right)}\left\{\emptyset_3\left[\frac{1}{2}Prf_1 f_5 + \frac{Br}{\emptyset_4}f_3^2\right] + Br.Ha.f_2^2\right\} \tag{17}$$

and with the boundary conditions

$$f_1(0) = f_w,\quad f_2(0) = 1 - r,\quad f_4(0) = 1,\ f_2(\infty) = r,\quad f_4(\infty) = 0. \tag{18}$$

In order to integrate functions in equations (16) and (17) as an initial value problem, we need the values of $f_3(0) := p$ and $f_5(0) := q$ that is $f''(0)$ and $g'(0)$, respectively. Our aim in this paper is to get the surface drag and the wall heat transfer rate for the various values of the physical parameters.

One of the most important tasks in shooting method is to obtain the appropriate finite values of η_∞. In order to determine η_∞ for the boundary value problem stated by Equations (16) and (17), we start with some initial guess values for some particular set of physical parameters to obtain $f''(0)$ and $g'(0)$ differ by pre-assigned significant digits. Finally, the last value of η_∞ is chosen to be the most appropriate value of the limit η_∞ for that particular set of parameters. The value of η_∞ may change for other set of physical parameters. Once the finite value of η_∞ is determined, then the integration is carried out [21].

Table-1. Thermophysical properties of water, copper and Alumina, Ahmad, et al. [5]

Physical Quantity	Properties		
	$\rho(kg/m^3)$	C_p(J/kgK)	k(W/mK)
Pure water	997.1	4179	0.613
Cu	8933	385	400
Al_2O_3	3970	765	40

Table-2. Comparisons of $(Re_x)^{1/2}C_f$ with that of Motsumi and Makinde [15] for various values of $\emptyset$ when $Br = 0$, $Ha = f_w = 0$, $R = \infty$, $r = 1$ and $Pr = 6.2$.

	Cu – water		Al_2O_3 – water	
$\emptyset$	Motsumi and Makinde [15]	Present Work	Motsumi and Makinde [15]	Present Work
0	0.3321	0.332057	0.3321	0.332057
0.008	0.3459	0.345921	0.3394	0.339385
0.014	0.3563	0.356293	0.3449	0.344943
0.016	0.3597	0.359747	0.3468	0.346808
0.02	0.3667	0.366654	0.3506	0.350557
0.1	0.5076	0.507634	0.4316	0.431592
0.2	0.7066	0.706563	0.5545	0.554510

Accordingly, the initial condition vector for the boundary value problem is given by $[f(0), f'(0), f''(0), g(0), g'(0)]$, that is $Y_0 = [f_w, 1-r, p, 1, q]$.We found the values of $f''(0)$ and$-g'(0)$ applied for the fourth order Runge – Kutta integration scheme with step size $h = 0.01$ for the various properly chosen physical parameters involved in the equations. The above procedures were repeatedly performed till we obtained the desired degree of accuracy, 10^{-6}.

4. RESULTS AND DISCUSSION

We considered two types of water-based nanofluids containing nanoparticles of Cu and Al_2O_3. For comparison purposes, we chose the Prandtl number Pr to be 6.2 (for Table 2 calculations only) and the nanoparticle volume fraction is investigated in the range $0 \leq \emptyset \leq 0.2$. According to Ahmad, et al. [5], we considered the thermophysical properties of water, copper and alumina for numerical calculations as shown in Table 1.

In the numerical solutions, the effects of magnetic field, viscous dissipation and thermal radiation on boundary-layer flow of water-based nanofluids over a moving permeable flat plate were considered. The transformed nonlinear ordinary differential equations (10) and (11) subjected to the boundary conditions (12) were solved numerically using the shooting technique followed by the Runge–Kutta method. Velocity and temperature profiles were obtained and we applied the results to compute the skin friction coefficient and the local Nusselt number. The numerical results were discussed for the various values of the embedded parameters graphically and in table form. To validate the accuracy of the numerical results, comparisons were made with Motsumi and Makinde [15] in the absence of viscous dissipation and magnetic field; as shown in Table2, the results are in excellent agreement and so it ensures us as a benchmark for the accuracy of the numerical results.

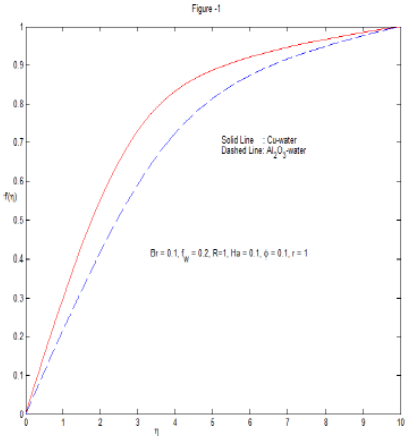

Fig-1. Blasius velocity profile

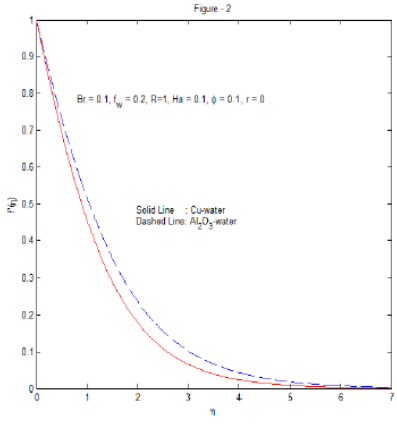

Fig-2. Sakiadis velocity profile

When $r = Ha = f_w = 0$, $R = \infty$, $r = 1$ and $Pr = 6.2$ for different values of nanoparticle volume fraction $\emptyset$, the term $(Re_x)^{1/2}C_f$ is calculated and excellent agreements are noticed for both nanofluids . In the following subsections, we pointed out the effects of the various thermophysical parameters on the nanofluid velocity and temperature profiles as well as the skin friction and the local Nusselt number on the plate surface. The Prandtl number Pr = 6.785 for pure water was considered in the succeeding numerical calculations.

Fig.1 and Fig.2 show the *Blasius* (the flow over the stationary plate is driven by free stream velocity alone) and *Sakiadis (the flow due to motion of the plate alone)* velocity profiles for both nanofluids which occur when $r = 1$ and $r = 0$, respectively. It is observed that the Cu-water nanofluid produced thicker momentum boundary layer thickness than that of Alumina in the case of Blasius velocity profile and the opposite is true in the case of Sakiadis velocity profile. Fig.3 shows the effects of velocity ratio parameter r on velocity profile of the Alumina nanofluid. As mentioned above, $r = 0$ and $r = 1$ are Sakiadis and Blasius velocity scenarios, respectively. When $r = 0.5$, both the plate and the free stream move with the same velocity. On the other hand, if $r = 1.5$, the plate and the free stream move in opposite directions.

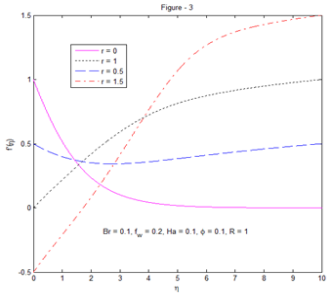

Fig-3. Effects of r on velocity profile of Alumina Nanofluid

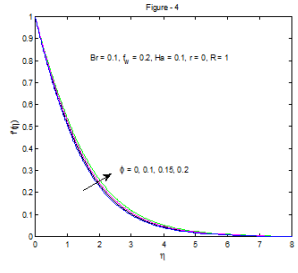

Fig-4. Effects of Ø on Sakiadis velocity profile Alumina Nanofluid

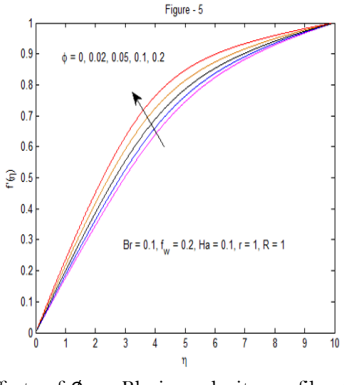

Fig-5. Effects of Ø on Blasius velocity profile of Alumina Nanofluid

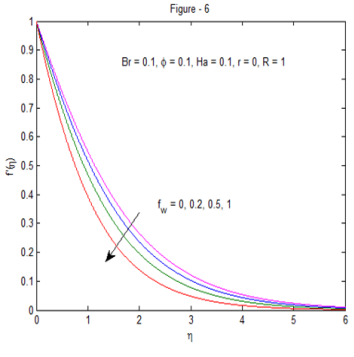

Fig-6. Effects of f_w on Sakiadis velocity profile of Alumina Nanofluid

Fig.4, Fig.6 and Fig.8 illustrate the effects of nanoparticle volume fraction $\emptyset$, the suction parameter f_w and the magnetic parameter Ha on the velocity profile of Alumina nanofluid when the velocity ratio parameter r is 0. We found the momentum boundary layer thickness slightly increases as the nanoparticle volume fraction of the nanofluid increases. On the other hand, the

momentum boundary layer thickness decreases as both the suction parameter and the magnetic parameter increase.

Fig.5, Fig.7 and Fig.9 depict the effects of nanoparticle volume fraction, the suction parameter and the Hartmann number on the velocity profile of Alumina nanofluid when r is 1. We investigated that the velocity boundary layer thickness increases as both the nanoparticle volume fraction and the suction parameter increase whereas it decreases as the magnetic parameter increases. It is an expected result that increasing nanofluid suction at the moving plate surface ($r = 0$), decreases the fluid velocity.

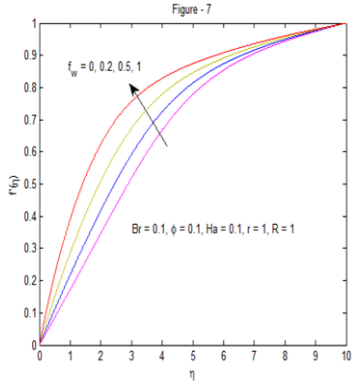

Fig-7. Effects of f_w on Blasius velocity profile of Alumina Nanofluid

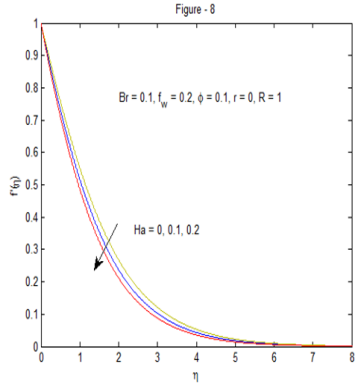

Fig-8. Effects of Ha on Sakiadis velocity profile of Alumina Nanofluid

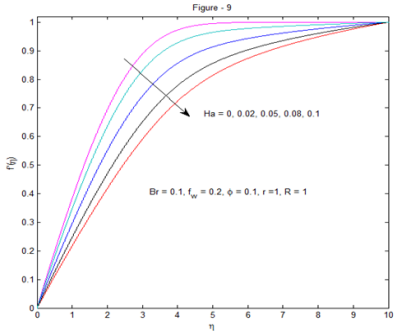

Fig-9. Effects of Ha on Blasius velocity profile of Alumina Nanofluid

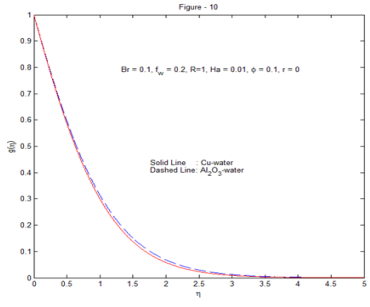

Fig-10. Sakiadis temperature profile of both nanofluids

Fig.10 describes the temperature profiles of the two nanofluids when motion of the fluid is caused by the motion of the plate alone ($r = 0$). It is observed that the thermal boundary layer thickness of Alumina water nanofluid is thicker than that of Cu-water nanofluid.

Figs.11-16 describe effects of the various parameters on temperature profiles of Alumina water nanofluid. As it is clearly shown in the figures, the temperature of the flow is highest at the plate surface and gradually declines to its zero free stream value far away from the plate.

Fig.11 shows the effects of velocity ratio parameter r on temperature profile of Alumina nanofluid. As the velocity ratio parameter increases from 0 to 1.5, the temperature rises within the boundary layer. This can be attributed to the fact that as r varies from 0 to1.5, the velocity of the plate declines to zero and then starts to move in the opposite direction of the free stream and

as a result of this, the internal heat generation within the nanofluid increases due to the nanoparticles and viscous dissipation.

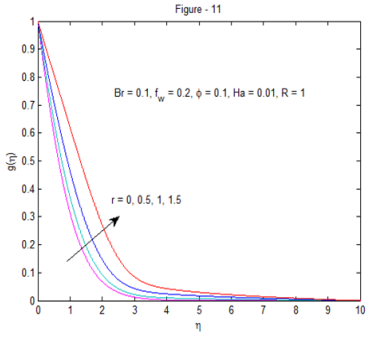

Fig-11. Effects of r on temperature profile for Alumina Nanofluid

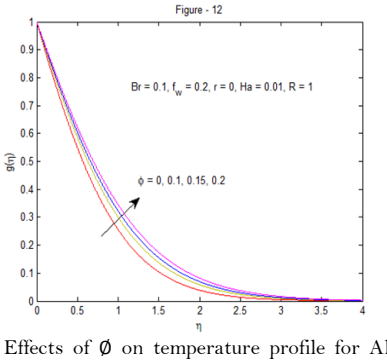

Fig-12. Effects of Ø on temperature profile for Alumina Nanofluid

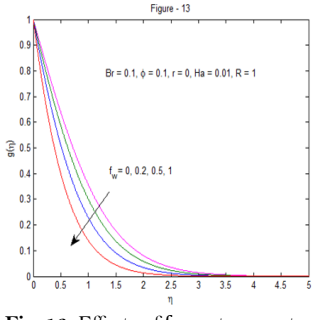

Fig-13. Effects of f_w on temperature profile for Alumina Nanofluid

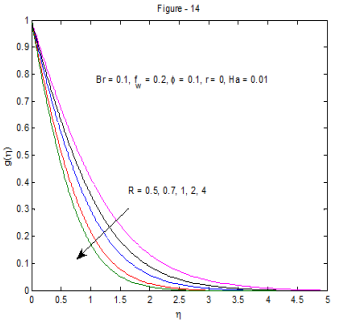

Fig-14. Effects of R on temperature profile for Alumina Nanofluid

Fig.12, Fig.15 and Fig.16 depict the effect of nanoparticle volume fraction, viscous heating and magnetic field on temperature profile and these parameters enhance in thickening the thermal boundary layer. On the other hand, Fig.13 and Fig.14 describe that both the suction parameter and thermal radiation parameters reduce the temperature profile. Table 3 shows the effect of nanoparticle volume fraction on skin friction and Nusselt number of Cu-water and Alumina water nanofluids. As the nanoparticle volume fraction increases, both skin friction and Nusselt number increase. As Ø increases, the skin friction of Cu-water nanofluid grows faster than that of Alumina. On the other hand, the Nusselt number of Alumina nanofluid increases slightly faster than that of Cu-water.

Table 4 shows the effect of magnetic parameter on skin friction and Nusselt number of both Cu-water and Alumina water nanofluids. As the magnetic parameter increases, the skin friction of both nanofluids increase but the opposite is true for the case of Nusselt number of both nanofluids.

Table-3. Comparisons of skin friction and Nusselt numbers of Cu-water and Al_2O_3-water nanofluids for various values of $\emptyset$

$Ha = 0.01,\ Br = 0.1,\ R = 1,\ Pr = 6.785,\ fw = 0.2,\ r = 1$				
$\emptyset$	Cu-water		Al_2O_3-water	
	$(Re_x)^{1/2}C_f$	$\frac{Nu_x}{\sqrt{Re_x}}$	$(Re_x)^{1/2}C_f$	$\frac{Nu_x}{\sqrt{Re_x}}$
0	0.380273	1.553388	0.380273	1.553388
0.016	0.417847	1.583000	0.398578	1.565829
0.02	0.427215	1.590041	0.403213	1.568893
0.1	0.616870	1.710688	0.501791	1.627104
0.2	0.875484	1.832657	0.646169	1.694550

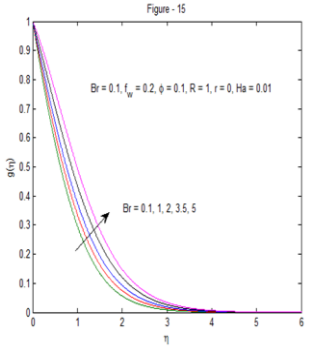

Fig-15. Effects of Br on temperature profile for Alumina Nanofluid

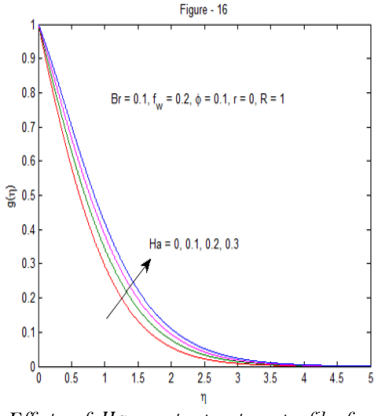

Fig-16. *Effects of Ha on temperature profile for* Alumina Nanofluid

Table-4. Comparisons of skin friction and Nusselt numbers of Cu-water and Al_2O_3-water nanofluids for various values of Ha

$\emptyset = 0.1,\ Br = 0.1,\ R = 1,\ Pr = 6.785,\ fw = 0.2,\ r = 0$				
Ha	Cu-water		Al_2O_3-water	
	$\lvert(Re_x)^{1/2}C_f\rvert$	$\left\lvert\frac{Nu_x}{\sqrt{Re_x}}\right\rvert$	$\lvert(Re_x)^{1/2}C_f\rvert$	$\left\lvert\frac{Nu_x}{\sqrt{Re_x}}\right\rvert$
0	0.788879	2.409460	0.656298	2.462345
0.01	0.797145	2.405563	0.666040	2.457706
0.1	0.868670	2.371774	0.749155	2.412629
0.2	0.942739	2.336715	0.833223	2.377632
0.3	1.011977	2.303946	0.910280	2.340598

Table 5 depicts that skin friction increases with an increase of the suction parameter fw and the skin friction starts to decline when the free stream is stationary while the plate is moving ($r = 0$) till it attains the minimum value when both the free stream and the plate move with the same velocity ($r = 0.5$) and then it starts to increase till the plate is stationary and the free stream is moving ($r = 1$).

Table-5. Comparisons of skin friction of Cu-water and Al_2O_3-water nanofluids for various values of r and fw

$\lvert(Re_x)^{1/2}C_f\rvert$ for Cu-water and Al_2O_3--water when $Ha = 0.01,\ Br = 0.1,\ R = 1,\ r = 1,\ \emptyset = 0.1$								
	Cu-water				Al_2O_3—water			
r	$fw = 0$	$fw = 0.2$	$fw = 0.5$	$fw = 1$	$fw = 0$	$fw = 0.2$	$fw = 0.5$	$fw = 1$
0	0.686948	0.797145	0.977714	1.313183	0.586944	0.666040	0.794196	1.030009
0.5	0.016084	0.017383	0.019241	0.022052	0.017529	0.018669	0.020305	0.022804
1	0.485584	0.616870	0.825517	1.196458	0.407697	0.501791	0.650430	0.913612
1.25	0.623403	0.845304	1.183353	1.765352	0.523924	0.683814	0.926530	1.342584
1.5	0.559913	0.972540	1.481141	2.300694	0.464407	0.772785	1.145419	1.738208

Table 6 describes the combined effects of the suction parameter fw and velocity ratio parameter r on the Nusselt number in the case of both nanofluids. Heat transfer rate at the plate surface decreases with increasing values of the velocity ratio parameter but it increases with increasing values of the nanofluid suction parameter. The heat transfer rate of Cu-water nanofluid is greater than that of Alumina when the free stream is not stationary and the plate is moving.

Table-6. Comparisons of Nusselt numbers of Cu-water and Al_2O_3-water nanofluids for various values of r and fw

$\left\lvert\frac{Nu_x}{\sqrt{Re_x}}\right\rvert$ for Cu-water and Al_2O_3-water when $\mathrm{Pr} = 6.785,\ Ha = 0.01,\ Br = 0.1,\ R = 1,\ \emptyset = 0.1$								
	Cu-water				Al_2O_3—water			
r	$fw = 0$	$fw = 0.2$	$fw = 0.5$	$fw = 1$	$fw = 0$	$fw = 0.2$	$fw = 0.5$	$fw = 1$
0	1.981443	2.405563	3.105290	4.403126	2.031394	2.457706	3.157223	4.447338
0.5	1.670232	2.116802	2.856907	4.224517	1.655970	2.098238	2.831091	4.185128
1	1.237811	1.710688	2.490659	3.910355	1.166485	1.627104	2.396354	3.809083
1.25	0.949108	1.450283	2.258939	3.701871	0.850425	1.331806	2.129778	3.575701
1.5	0.503208	1.127923	1.990953	3.459976	0.377286	0.964072	1.821386	3.311167

Table 7 shows that the Nusselt number of Alumina nanofluid decreases with increasing values of both the Brinkmann number (Br) and radiation parameter (R).

Table-7. Comparison of Nusselt numbers of Al_2O_3-water nanofluids for various values of Br and R

$\left\lvert\frac{Nu_x}{\sqrt{Re_x}}\right\rvert$ for Al_2O_3-water, when $Pr = 6.785,\ fw = 0.2, r = 0,\ Ha = 0.01,\ \emptyset = 0.1$				
Br	$R = 0.5$	$R = 1$	$R = 2$	$R = 4$
0	2.845261	2.487546	2.255567	1.876524
0.1	2.813582	2.457706	2.227044	1.852794
1	2.528469	2.189147	1.970331	1.639221
2	2.211677	1.890748	1.685094	1.401918
3.5	1.736489	1.443150	1.257239	1.045963

5. CONCLUSIONS

The problem of a steady MHD boundary-layer flow of water-based nanofluids over a moving permeable flat plate has been analyzed. The governing PDEs associated to the boundary

conditions were transformed to non-linear ODEs with similarity transformation equations. The solutions of these problems were numerically solved with the help of the shooting technique followed by the fourth order Runge-Kutta integration technique. Among the others, the following substantial results are given below:

- The velocity profile decreases with an increase in the magnetic parameter whereas it increases as both the nanoparticle volume fraction and the suction parameters increase; but with the exception that the Sakiadis velocity profile decreases with the increment of the suction parameter.
- For Sakiadis flow scenario, Alumina water nanofluid exhibits thicker velocity boundary layer than that of Cu-water nanofluid.
- The thermal boundary layer thickness increases with increasing values of nanoparticle volume fraction, the Brinkmann number, the velocity ratio parameter and the magnetic parameter but it decreases with increasing values of both suction rate and thermal radiation parameters.
- Increasing the values of magnetic parameter, the suction rate parameter and nanoparticle volume fraction results in an increase in the skin friction coefficient. It is observed that the Cu-water nanofluid exhibits larger values of skin friction coefficient than that of Alumina.
- The presence of magnetic parameter, velocity ratio parameter, the Brinkmann number and radiation parameter in the flow field is to reduce the rate of thermal boundary layer thickness whereas suction parameter and nanoparticle volume fraction enhance thermal boundary layer thickness.

Funding: This study received no specific financial support.

Competing Interests: The authors declare that they have no conflict of interests.

Contributors/Acknowledgement: All authors contributed equally to the conception and design of the study.

REFERENCES

[1] A. B. Ahmadreza, "Application of nanofluid for heat transfer enhancement," *PID: 2739168, EEE-5425*, 2013.

[2] J. Buongiorno, "Convective transport in nanofluids," *J. of Heat Trans. Amer. Soci. of Mech. Engineers*, vol. 128, pp. 240-250, 2005.

[3] N. Bachok, A. Ishak, and I. Pop, "Boundary layer flow of nanofluids over a moving surface in a flowing fluid," *Int. J. of Thermal Sciences*, vol. 49, pp. 1663-1668, 2010.

[4] P. O. Olanrewaju, M. A. Olanrewaju, and A. O. Adesanya, "Boundary layer flow of nanofluids over a moving surface in a flowing fluid in the presence of radiation," *Int. J. of Appl. Sci. and Tech.*, vol. 2, pp. 274-285, 2012.

[5] S. Ahmad, A. M. Rohni, and I. Pop, "Blasius and Sakiadis problems in nanofluids," *Acta Mechanical*, vol. 218, pp. 195-204, 2011.

[6] F. M. Hady, R. E. Mohamed, M. R. Abd-Elsalam, and A. A. Mostafa, "The Blasius and Sakiadis flow in a nanofluid through a porous medium in the presence of thermal radiation under a convective surface boundary condition," *IJEIT*, vol. 3, pp. 225-234, 2013.

[7] O. D. Makinde and A. Aziz, "Boundary layer flow of a nanofluid past a stretching sheet with a convective boundary condition," *Int. J. of Thermal Sci.*, vol. 50, pp. 1326-1332, 2011.

[8] M. D. Khan, I. Karim, L. E. Ali, and A. Islam, "Unsteady MHD free convection boundary-layer flow of a nanofluid along a stretching sheet with thermal radiation and viscous dissipation effects," *Int. Nano Letters*, vol. 2, pp. 24. Available: http://www.inl-journal.com/content/2/1/24, 2012.

[9] M. A. A. Hamad, I. Pop, and A. I. M. Ismail, "Magnetic field effects on free convection flow of a nanofluid past a vertical semi-infinite flat plate," *Nonlinear Anal. Real World Appl.*, vol. 12, pp. 1338-1346, 2011.

[10] M. A. A. Hamad and I. Pop, "Scaling transformations for boundary layer flow near the stagnation-point on a heated permeable stretching surface in a porous medium saturated with a nanofluid and heat generation/ absorption effects," *Transport in Porous Media*, vol. 87, pp. 25-39, 2011.

[11] F. M. Hady, F. S. Ibrahim, S. M. Abdel-Gaied, and R. Eid Mohamed, "Radiation effect on viscous flow of a nanofluid and heat transfer over a nonlinearly stretching sheet," *Nanoscale Res. Letters*, vol. 7, p. 229. Available: http://www.nanoscalereslett.com/content/7/1/229, 2012.

[12] V. Rajesh, "Radiation effects on MHD free convective flow near a vertical plate with ramped wall temperature," *Int. J. of Appl. Math. and Mech.*, vol. 6, pp. 60-77, 2010.

[13] K. Jafar, R. Nazar, and A. Ishak, "MHD flow and heat transfer over stretching/shrinking sheets with external magnetic field, viscous dissipation and Joule effects," *Canadian J. Chem. Eng.*, vol. 90, pp. 1336-1346, 2012.

[14] K. Vajravelu and A. Hadjinicolaou, "Heat transfer in a viscous fluid over a stretching sheet with viscous dissipation and internal heat generation," *Int. Comm. Heat Mass Trans.*, vol. 20, pp. 417-430, 1993.

[15] T. G. Motsumi and O. D. Makinde, "Effects of thermal radiation and viscous dissipation on boundary layer flow of nanofluids over a permeable moving flat plate," *Phys.Scr.*, vol. 86, pp. 1-8, 2012.

[16] E. Hail and B. Shankar, "Magnetohydrodynamic nanofluid flow of a stretching sheet with thermal radiation, viscous dissipation, chemical reaction and ohmic effects," *J. of Nanofluids*, vol. 3, pp. 227-237, 2014.

[17] R. K. Tiwari and M. N. Das, "Heat transfer argumentation in a two sided lid-driven differentially heated square cavity utilizing nanofluids," *Int. J. Heat Mass Trans.*, vol. 50, pp. 2002-2018, 2007.

[18] A. Raptis, "Radiation and free convection flow through a porous medium," *Int. Comm. In Heat and Mass Tran.*, vol. 25, pp. 289-295, 1998.

[19] M. A. Hossain and H. S. Takhar, "Radiation effect on mixed convection along a vertical plate with uniform surface temperature," *Heat Mass Transf.*, vol. 31, pp. 243-248, 1996.

[20] E. Haile and B. Shanker, "Heat and mass transfer through a porous media of MHD flow of nanofluids with thermal radiation, viscous dissipation and chemical reaction effects," *Amer. Chem. Sci. J.*, vol. 4, pp. 828-846, 2014.

[21] I. C. Mandal and S. Mukhopadhyay, "Heat transfer analysis for fluid flow over an exponentially stretching porous sheet with surface heat flux in porous medium," *Ain Shams Eng. J.*, vol. 4, pp. 103-110, 2013.